Redox Biology 32 (2020) 101514

Contents lists available at ScienceDirect

Redox Biology

journal homepage: www.elsevier.com/locate/redox

Exogenous spermine attenuates rat diabetic cardiomyopathy via suppressing ROS-p53 mediated downregulation of calcium-sensitive receptor

Yuehong Wang[a], Junting Chen[b], Siwei Li[a], Xinying Zhang[a], Zuoming Guo[c], Jing Hu[a], Xiaoting Shao[a], Ningyang Song[a], Yajun Zhao[a], Hongzhu Li[a], Guangdong Yang[d], Changqing Xu[a], Can Wei[a,*]

[a] Department of Pathophysiology, Harbin Medical University, Harbin, 150081, China
[b] Department of Anesthesiology, The Fourth Affiliated Hospital of Harbin Medical University, Harbin, 150000, China
[c] Department of Hepatobiliary and Pancreatic Surgery, Harbin Medical University Cancer Hospital, Harbin, 150081, China
[d] Department of Chemistry and Biochemistry, Laurentian University, Sudbury, P3E 2C6, Canada

ARTICLE INFO

Keywords:
Calcium sensitive receptor
Diabetic cardiomyopathy
ER stress
Nrf2-ROS-p53-MuRF1 axis
Spermine
Unfolded protein response

ABSTRACT

Diabetic cardiomyopathy (DCM) is a severe complication of type 1 diabetic (T1D) patients, manifested as combined diastolic and systolic dysfunction. DCM is associated with impaired calcium homeostasis secondary to decreased calcium-sensitive receptor (CaSR) expression. Spermine, a direct agonist of CaSR, was found deficient in cardiomyocytes of T1D rats. However, the role of spermine in DCM was unclear. Here, we examined the cardioprotective effect of exogenous spermine on DCM in streptozotocin (STZ) induced-T1D rats and high-glucose (HG)-incubated neonatal rat cardiomyocytes. Exogenous spermine significantly attenuated cardiac dysfunction in T1D rats, characterized by improved echocardiography, less fibrosis, reduced myocardial endoplasmic reticulum (ER) stress and oxidative stress, and increased expression of myocardial membrane CaSR. In cultured neonatal rat cardiomyocytes, exogenous spermine attenuated myocardial injury induced by HG treatment, demonstrated by restored cellular glucose uptake capacity, reduced expression of apoptotic markers, lowered level of oxidative stress, ER stress and unfolded protein response, and upregulated cell membrane CaSR. Mechanistically, the cardioprotective effect of spermine appeared dependent upon effective elimination of reactive oxygen species (ROS) and up-regulation of CaSR expression by suppressing the Nrf2-ROS-p53-MuRF1 axis. Taken together, these results suggest that exogenous spermine protects against DCM *in vivo* and *in vitro*, partially via suppressing ROS and p53-mediated downregulation of cell membrane CaSR.

1. Introduction

The pathogenesis of type 1 diabetes (T1D) has not been well understood [1,2]. Diabetes mellitus can result in direct damage to the structure and function of myocardium without causing vascular disease such as hypertension or coronary artery disease, a condition known as diabetic cardiomyopathy (DCM). DCM is one of the most severe complications of T1D, characterized by combined diastolic and systolic cardiac dysfunction [3,4]. However, the exact mechanism of myocardial dysfunction caused by DCM has not been well understood.

Myocardial dysfunction is associated with impairment of myocardial energy metabolism and calcium homeostasis [5,6]. We have previously reported that down-regulation of myocardial calcium-sensitive receptor (CaSR) protein in DCM rats resulted in the decrease of intracellular calcium concentration and deteriorated high glucose (HG)-induced energy metabolism disorder in cardiomyocytes [6,7]. CaSR is a member of the G-protein coupled receptor C family and is ubiquitously expressed in various tissues. In cardiomyocytes, CaSR plays a key role in energy metabolism, ischemia reperfusion injury and regulation of calcium homeostasis [6–8]. Reduced expression of CaSR leads to mitochondrial dysfunction, impairment of gap junctional intercellular communication, and ultimately energy insufficiency in cardiomyocytes [7]. Elucidating the precise mechanism by which CaSR downregulation will provide important insight into the potential therapeutic application against DCM.

Spermine, a small polyamine, is a natural products of cellular metabolism found in all eukaryotic cells. Spermine regulates cell proliferation, differentiation and apoptosis, etc [9,10]. We have previously found that the intracellular content of spermine was decreased significantly in cardiomyocytes of T1D rats [6]. Furthermore, it has been

* Corresponding author. Department of Pathophysiology, Harbin Medical University, Baojian Road, Harbin, 150081, China.
E-mail address: canwei528@163.com (C. Wei).

https://doi.org/10.1016/j.redox.2020.101514
Received 11 December 2019; Received in revised form 23 February 2020; Accepted 18 March 2020
Available online 21 March 2020

Abbreviations used

2DG	2-Deoxy-D-Glucose
4-PBA	4-phenylbutyric acid
ATF	activating transcription factor
CaSR	calcium-sensitive receptor
CAT	catalase
CK-MB	creatine kinase isoenzyme
cTnT	cardiac troponin
DCF	2'-7'-dichloroflorescein
DCM	diabetic cardiomyopathy
ER	endoplasmic reticulum
Ero1	ER oxidoreductin 1
GSP	glycated serum protein
HG	high glucose
Hsp	heat shock protein
IRE1	inositol-requiring enzyme 1
LDH	lactate dehydrogenase
MDA	malondialdehyde
MDM	murine double microsomes
Mn-SOD	manganese superoxide dismutase
MuRF1	muscle-specific ring finger protein 1
NAC	N-acetyl cysteine
Nrf2	nuclear factor erythroid 2-related factor 2
OAZ	ODC antizyme
ODC	ornithine decarboxylase
PDI	protein disulfide isomerase
PI	propidium iodide
ROS	reactive oxygen species
SSAT	spermidine/spermine N1-acetyltransferase
STZ	streptozotocin
T1D	type 1 diabetes
TEM	transmission electron microscopy
UPR	unfolded protein response

reported that spermine could directly activate CaSR as a multivalent cation, implicating a potential role of spermine in regulating CaSR function and signaling [7].

Here, we hypothesize that exogenous spermine regulates CaSR function *in vivo and in vitro*. We examined the effect of exogenous spermine on DCM in streptozotocin (STZ) induced-T1D rats and HG-incubated neonatal rat cardiomyocytes. Our results revealed that exogenous spermine could upregulate myocardial membrane CaSR expression, and protected against DCM in T1D rats and HG-injured cardiomyocytes.

2. Materials and methods

2.1. Experimental animals

Male wistar rats (200–250 g) were purchased from the Experimental Animal Center of Second Affiliated Hospital of Harbin Medical University (Harbin, China) and bred at the Animal Reproduction Facility of the Department of Pathophysiology of Harbin Medical University. T1D group was induced by a single intraperitoneal injection of 60 mg/kg STZ. The drug was dissolved in 0.1 M citric acid-citrate sodium buffer (pH 4.5). Control group (Control) were injected with the same volume of buffer only. Spermine group (Sp) were injected with spermine (2.5 mg/kg/day) every day for two weeks prior to STZ injection, after that, spermine (2.5 mg/kg/day) was injected every other day for 12 weeks. Experimental rats were fasted 12 h prior to the STZ administration; immediately thereafter, 10% sucrose was supplemented in the drinking water for 24 h to avoid sudden hypoglycemia due to insulin hyper-secretion. Animal safety protocols for the use of STZ in rodents were followed by the investigators and the Animal Laboratories personnel according to the guidelines of the Harbin Medical University. The body weight and blood glucose levels were monitored once weekly after 6 h fasting. All rats were housed in a vivarium with humidified airflow and a 12:12 h light-dark cycle at a constant temperature of 24 °C. Water and food were provided ad libitum.

2.2. Animal echocardiography

Echocardiography was carried out at 1 day before and 12 weeks after STZ injection. Animals were anesthetized under 3% pentobarbital sodium and standard two-dimensional echocardiographic left ventricular parameters were obtained from the parasternal short and long axis [6]. All settings were optimized to obtain maximal signal-to-noise ratio and two-dimensional images to provide optimal endocardial delineation.

2.3. Serum and tissue preparation

After 12 weeks, the animals were fasted overnight and then anesthetized with pentobarbital sodium for blood and tissue collection. Blood samples were collected into tubes containing an anticoagulant. The heart was carefully dissected from the surrounding tissues and cut into three parts. One part of tissue samples were fixed with 4% polyformaldehyde, then embedded in paraffin and dehydrated in gradient sucrose for hematoxylin-eosin (H&E) staining, Sirius red staining, masson staining, and immunofluorescent staining. A second part of tissues was fixed with 2.5% glutaraldehyde for observation with transmission electron microscope. The third part of tissues was stored at −80 °C for further experiments.

2.4. Measurement of enzymatic activities

The stored myocardial tissues were homogenized in ice cold phosphate buffer. Then the homogenate was centrifuged at 3000 × *g* for 15 min. Manganese superoxide dismutase (Mn-SOD or SOD2), malondialdehyde (MDA) and catalase (CAT) in the supernatant were measured by using ELISA kits (Elabscience, Wuhan, China). Cardiac troponin (cTnT), lactate dehydrogenase (LDH), creatine kinase isoenzyme (CK-MB) and glycated serum protein (GSP) in the blood serum were measured by using commercially available kits (Jiancheng Institute of Bioengineering, Nanjing, China). All assays were conducted according to the manufacturer's instructions.

2.5. Histological assay

The myocardial ultrastructure and DCM lesions were evaluated using H&E staining and observed under a microscope. Masson's trichrome staining and sirius red staining were performed to assess the collagen contents in heart tissue. Immunofluorescent staining were analyzed using a computer-assisted color image analysis system (Image-Pro Plus, version 6.0, Media Cybernetics, Inc., Silver Spring, MD, USA) as previously described [6,11].

2.6. Isolation and culture of neonatal rat cardiomyocytes

Primary cultures of cardiomyocyte from neonatal wistar rat (1–3 days old) were prepared as previously described [6]. Briefly, the hearts were cut into pieces and digested with trypsin (Beyotime Biotechnology, Shanghai, China) for 8 min, then DMEM culture medium was added to terminate the digestion. After 8 times of the same process, the cells were collected by centrifugation at 600 × *g* at 4 °C for 10 min and then incubated with DMEM in a humidified atmosphere at 37 °C

with 5% CO_2 for 2 h. After that, the attached cells were discarded and the unattached cardiomyocytes were replated in collagen-coated petri dish containing 10% fetal bovine serum (FBS) and 1% penicillin or streptomycin. The media was changed every 2–3 days.

2.7. Cardiomyocyte treatments

The cultured neonatal rat cardiomyocytes were treated with 9 different groups as described below. (1) Control group: normal DMEM medium with a glucose concentration of 5.56 mmol/L; (2) Control + spermine (Control + Sp) group: the cells were treated with 5.56 mmol/L glucose and 5 μmol/L spermine for 48 h; (3) High glucose (HG) group: the cells were treated with 40 mmol/L glucose for 48 h; (4) HG + Sp group: the cells were treated with 40 mmol/L glucose and /L and 5 μmol/L spermine for 48 h; (5) HG + ER stress inhibitor (HG + 4-PBA) group: the cells were treated with 40 mmol/L glucose and 0.5 mmol/L 4-PBA for 48 h; (6) HG + PERK inhibitor (HG + GSK2606414) group: the cells were treated with 40 mmol/L glucose and 40 nmol/L GSK2606414 for 48 h; (7) HG + IRE1 inhibitor (HG + STF-083010) group: the cells were treated with 40 mmol/L glucose and 50 μmol/L STF-083010 for 48 h; (8) HG + ATF6 inhibitor (HG + AEBSF HCl) group: the cells were treated with 40 mmol/L glucose 100 μmol/L AEBSF HCl for 48 h; (9) HG + N-Acetyl Cysteine (NAC) treatment (HG + NAC) group: the cells were treated with 40 mmol/L glucose and 5 mmol/L NAC for 48 h.

2.8. Electron microscopy analysis

Heart tissues or collected primary cultured neonatal cardiomyocytes were fixed in 2.5% glutaraldehyde, followed by 1% osmium tetroxide. Then, tissues were dehydrated in a series of alcohols and finally embedded. Ultrastructural changes of cardiomyocytes were observed under an electron microscope.

2.9. Glucose uptake in cardiomyocytes

Glucose uptake assay was measured with 96-well low adherent white luminescent plates. Prior to the assay, the culture medium was removed and the cells were washed with 100 μL of phosphate-buffered saline (PBS). To initiate glucose uptake, 50 μL of 2-Deoxy-D-Glucose (2DG, 1 mmol/L) in PBS was added to cells for 60 min. The uptake reaction was then stopped and samples were processed as described in the standard protocol of the Glucose Uptake Glo Assay kit (Promega, Madison, WI, USA). Luminescence was read with 0.3–1 s integration on a luminometer (Thermo Fisher Scientific, Scotland, UK) and the rate of glucose uptake was expressed as fmol/min/cell.

2.10. Neutral comet assay

DNA damage was analyzed with single cell gel electrophoresis by using the Trevigen CometAssay kit (Trevigen, Gaithersburg, MD, USA) according to the manufacturer's instructions. In brief, the cells were washed and digested and then centrifuged at 200×*g* for 5 min. Approximately 2 × 10^5 cells were resuspended in 0.1% low-melting point agarose (LMAgarose). A volume of 50 μL of the cell suspension was pipetted onto designated areas of CometSlides and allowed to solidify for 30 min at 4 °C. The cells were lysed in CometAssay Lysis Solution for 1 h in the dark at 4 °C. Samples were immersed in 1 × Neutral Electrophoresis Buffer for 30 min at 4 °C and then transferred to an electrophoresis unit for separation under 21 V for 45 min at 4 °C. The slides were removed from the unit and placed in DNA precipitation solution (7.5 mmol/L NH_4Ac in 95% ethanol) for 30 min at room temperature in the dark. Afterward, the slides were transferred into 70% ethanol for an additional 30 min at room temperature in the dark. The slides were subsequently dried at 37 °C in the dark for 15 min and then stained with SYBR Green I stain (Invitrogen) in Tris-EDTA buffer (pH 7.5). The comets were visualized under an Axioplan 2 IE fluorescent microscope equipped with an AxioCam MRm digital camera (Zeiss). Images were captured using AxioVision 4.8 software (Zeiss). The tail length from at least 50 nuclei per experimental group was determined using ImageJ software (NIH) with the Comet Assay plug-in. Statistical significance of comet assay results was determined using a nonparametric Mann-Whitney *U* test.

2.11. Immunofluorescence assay

After treatments, cardiomyocytes seeded in glass slides washed, fixed, and permeabilized. Then, the cells were immunolabelled with specific primary antibodies (CaSR and calnexin at 1:50 ratio) overnight at 4 °C. After rinsing, the cells were incubated with corresponding fluorescent-conjugated secondary antibody (goat anti-mouse IgG and goat anti-Rabbit IgG; Rockland Immunochemicals Inc, Limerick, PA) plus DAPI nuclear counterstain or Wheat Germ Agglutinin cytomembranes counterstain, and then observed using a microscope with fluorescence objectives (Olympus I×51, Center Valley, PA).

2.12. Annexin V/PI detection of apoptosis and flow cytometric analysis of ROS

Annexin V-FITC/propidium iodide (PI) Apoptosis Detection Kit (BD Pharmingen, Franklin Lakes, NJ, USA) was used to detect apoptosis according to the manufacturer's instructions. Briefly, the cells were collected and incubated with 5 μL Annexin V-FITC and 10 μL PI for 15 min at room temperature in the dark. After filtration, the cells were analyzed by fluorescence-activated cell sorting Calibur system within 1 h. Annexin V^+/PI^- and Annexin V^+/PI^+ represent the apoptotic cells in early and late phase, respectively. The level of ROS was evaluated by using the fluorescence intensity of 2'-7'-dichloroflorescein (DCF). The cells were incubated with DMEM medium containing 20 μmol/L DCFH-DA for 30 min at 37 °C in the dark. After rinsing, digesting and filtration, the cells were analyzed by fluorescence-activated cell sorting Calibur system within 1 h. All data were analyzed using BD GACSDiva Software v7.0 (Becton-Dickinson, USA).

2.13. Plasmid construction and cell transfections

Adenovirus vectors containing MuRF1 and PPARα were purchased from Shanghai GenePharma (Shanghai, China). Cardiomyocytes were seeded at equal number of cells (2.0 × 10^5 per dish) in 35 mm petri dish and maintained in the absence of antibiotic culture medium for 24 h before transfection. The viral solution was diluted with reduced serum media (GibcoTM Opti-MEMTM, Thermo Fisher Scientific, UK) at 1:50. After the cells were transfected with adenovirus vector at 37 °C for 24 h, reduced serum DMEM medium was discarded. Another 2 mL fresh culture medium containing 10% FBS was added to each dish for 48 h with various treatments.

2.14. siRNA transfection

Cardiomyocytes were seeded at equal number of cells (2.0 × 10^5 per dish) in 35 mm petri dish and maintained in the absence of antibiotic culture medium for 24 h before transfection. Cardiomyocytes were transfected with scrambled-siRNA or gene-specific siRNA (Santa Cruz Biotechnology, TX, USA) using Lipofectamine™ 3000 transfection reagent from Invitrogen (Thermo Fisher Scientific, Scotland, UK). The transfection reagent complex was added to the reduced serum media (GibcoTM Opti-MEMTM, Thermo Fisher Scientific, UK) for 8 h, the transfection was continued for another 24 h in serum-containing normal medium.

2.15. Plasma membrane protein fractionation

Plasma membrane and organelles enriched fractions were isolated with differential density centrifugation by using a commercial kit (Invent Biotechnologies, Plymouth, MN, USA). The purity of each fraction was validated by western blotting using specific antibodies.

2.16. Immunoblotting

Total protein from cardiomyocytes and heart tissue was extracted by using Minute™ Total Protein Extraction Kit (Invent Biotechnologies, Plymouth, MN, USA). After quantification and denaturation, equal amounts of protein samples were electrophoresed in SDS-polyacrylamide gel and transferred onto PVDF membranes (Millipore, Schwalbach, Germany). The following primary antibodies were used in this experiment: nuclear factor erythroid 2-related factor 2 (Nrf2), SOD2, heat shock protein (Hsp) 70, Hsp90, Grp78, Grp94, p53, murine double microsomes (MDM) 2, MDM4, muscle-specific ring finger protein 1 (MuRF1), p-PERK, p-eIF2α, activating transcription factor (ATF) 4, inositol-requiring enzyme 1 (IRE1), XBP-1, CHOP, Cleaved-ATF6, β-actin, β-tubulin, Na^+-K^+-ATPase and Histone H3 from Proteintech, Wuhan, China; Pro-Caspase3, Cleaved-Caspase3, Pro-Caspase9, Cleaved-Caspase9 and ER oxidoreductin 1 (Ero1) from Cell Signaling Technology, MA, USA); CaSR, ornithine decarboxylase (ODC) and spermidine/spermine N1-acetyltransferase (SSAT) from Santa Cruz Biotechnology; protein disulfide isomerase (PDI) from Enzo Life Sciences, Lausen, Switzerland; PPARα from Abcam, Cambridge, UK. The CaSR, ODC and SSAT antibody were diluted 1:250, the other primary antibodies were diluted 1:1000 and incubated with the membrane overnight at 4 °C. Subsequently, a 1:10000 dilution of the secondary antibody (ZSGB-BIO, Beijing, China) was added to the membrane. The signals were detected by the Enhanced Chemiluminescent (ECL) kit (HaiGene, Harbin, China) and the Multiplex Fluorescent Imaging System (ProteinSimple, California, USA). The intensities of protein bands were quantified by a Bio-Rad ChemiDocTM EQ densitometer and Bio-Rad Quantity One software (Bio-Rad Laboratories, Hercules, CA, USA) and normalized to Na^+-K^+-ATPase, Histone H3, β-actin or β-tubulin, individually.

2.17. Immunoprecipitation

Immunoprecipitation was performed as previously described [6]. Briefly, after centrifugation at 14000 × *g* for 20 min, the lysates were immunoprecipitated with 2 μg of antibody against MDM4 (Cell

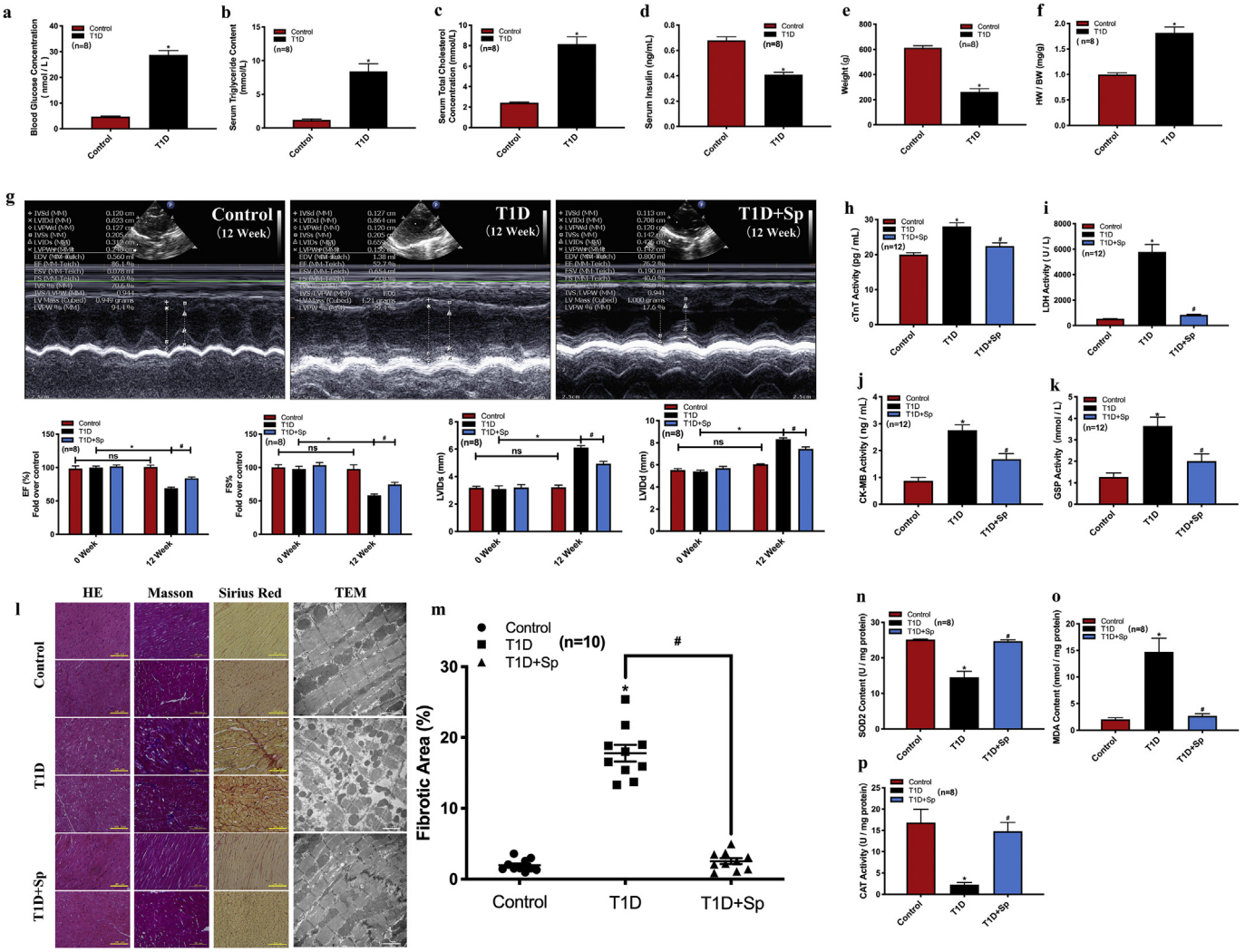

Fig. 1. Exogenous spermine inhibits STZ-induced myocardial injury in DCM rats. STZ (60 mg/kg) was injected into the abdominal cavity of rats to establish the model of T1D and the related indexes were determined 12 weeks later. (a) blood glucose concentration, (b) serum triglyceride concentration, (c) serum cholesterol concentration, (d) serum insulin concentration, (e) body weight, (f) heart weight/body weight, (g) cardiac function, (h) serum cTnT concentration, (i) serum LDH concentration, (j) serum CK-MB concentration, (k) serum GSP concentration, (l) myocardial histomorphology, (m) myocardial fibrosis level, (n) SOD2 concentration, (o) MDA concentration, and (p) CAT concentration were detected. *, P < 0.05 versus Control group; #, P < 0.05 versus T1D group.

Signaling Technology) overnight at 4 ˚C followed coupling to Protein A/G Magnetic Beads (Selleckchem, Houston, TX, USA) for 2 h. The immunoprecipitated samples were resolved on SDS-PAGE and subjected to Western blot analysis with specific antibodies.

2.18. Quantitative real-time PCR (qRT-PCR)

Samples from animals and cells were used for qRT-PCR analysis with a cDNA kit (Bimake, Houston, TX, USA) according to the manufactures's instructions. qRT-PCR was performed by using SYBR Green qPCR Master Mix with a Roche LightCycler 96 setup. The sequences of primers were used as follow: ODC (5'-TCTATGTTGCGGACCTCGGA GAC-3' and 5'- GTGCTCACTATGGCTCTGCTGTC-3'); SSAT (5'-TCTTG AATAGTCTCCATCCCTC-3' and 5'- AGCCAGGTTGCTATGAAGTGT-3'); OAZ1 (5'-ACTGCCGCATCCTCTTCCT-3' and 5'- TCAACGTCACACACTT CATGATGGA-3'); PDI (5'-CAACGTCCTGGTGCTGAAGAAGAG-3' and 5'-TGCTAGTCGGATCTCAGAGCCTTC-3'); CaSR (5'-TCCTACAATGTGTAC TTAGCCG-3' and 5'-AGGTGCCAGTTGATGATAGAAT-3'); Ero1α (5'-GGCTTGCTCGTCGGACTCTTG-3' and 5'-CGATGGTCTCGACATCACAG GTAC-3'); Ero1β (5'-GACGACTGTGAGCAGGCTAACAAG-3' and 5'-GGTTCAGCAGCAGGTCCACATAC-3'); MDM2 (5'-GCGAGCGGAGACGG ACACAC-3' and 5'-GGGCTCTGTGGCGCTTCCTC-3'); MDM4 (5'-TCAA ATTCCCTAGAAACCACC-3' and 5'-GATTCCAGAGCAGATGAAGACT-3'); p53 (5'- GAGGTCGGCTCCGACTATACCA-3' and 5'- AAAGCTGTCC CGTCCCAGAAG-3'); β-actin (5'-ATGGATGACGATATCGCTGC-3' and 5'-CTTCTGACCCATACCCACCA-3').

2.19. Statistical analysis

Statistical analyzes were performed using SPSS 21.0 software. All data are presented as means ± standard errors of the means (SEM). One-way analysis of variance (ANOVA) followed by the Student-Newman-Keuls test were used for statistical analyses of three or more groups. Student's t-test was applied to analyze statistically significant differences between two groups. A $p < 0.05$ was considered statistically significant. GraphPad Prism was used for mapping and curve fitting.

3. Results

3.1. Establishment of a DCM model in STZ-induced T1D rats

A single injection of STZ has been widely used to establish T1D model in rats [7,12]. STZ is an alkylating compound that selectively ablates pancreatic beta cells [12]. Here, we validated that a single intraperitoneal injection of STZ (60 mg/kg body weight) in rats resulted in metabolic phenotypes that are characteristics of human T1D, including marked increase of serum glucose, triglyceride, and cholesterol level, decreased serum insulin, and lower body weight (Fig. 1a–e). STZ-injected rats also developed common signs of T1D, including polydipsia, polyuria, and noticeable hypoactivity and weakness (data not shown). We next examined the cardiac function of T1D rats. The heart-to-weight ratio was significantly increased in T1D rats compared with control rats (Fig. 1f). Echocardiography revealed significantly impaired cardiac function 12 weeks after STZ delivery, as shown by decreased left ventricular ejection fraction (EF%), decreased fractional shortening (FS%), and increased left ventricular internal dimension (LVID) at end-systole (LVIDs) and end-diastole (LVIDd) (Fig. 1g). Taken together, these results showed that a DCM model was successfully established in STZ-induced T1D rats.

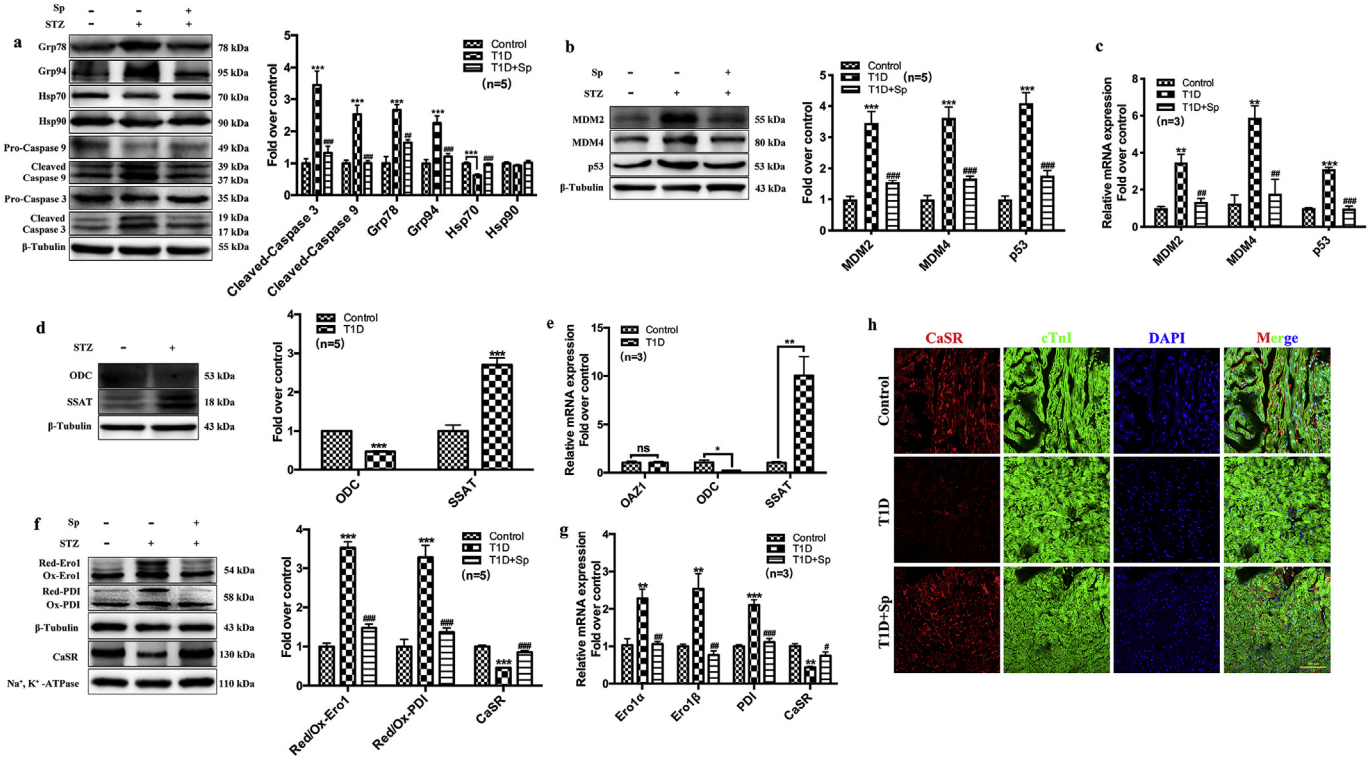

Fig. 2. Exogenous spermine up-regulates the expression of cytomembrane CaSR and inhibits cardiomyocytes injury in DCM rats. Twelve weeks after STZ injection in rats, (a) the expression of Grp78, Grp94, Hsp70, Hsp90, Cleaved-Caspase 9 and Cleaved-Caspase 3 were detected and quantified, (b) Quantification of MDM2, MDM4 and P53 protein expression, (c) Quantification of MDM2, MDM4 and P53 mRNA expression, (d) Quantification of ODC and SSAT protein expression change, (e) Quantification of OAZ1, ODC and SSAT mRNA expression change, (f) Quantification of Ero1, PDI and cytomembrane CaSR protein expression change, (g) Quantification of Ero1, PDI and cytomembrane CaSR mRNA expression change, (h) The expression of CaSR in myocardial tissue was detected by laser confocal. Scale bar = 200 μm *, P < 0.05 versus Control group; **, P < 0.01 versus Control group; ***, P < 0.001 versus Control group; #, P < 0.05 versus T1D group; ##, P < 0.01 versus T1D group; ###, P < 0.001 versus T1D group.

3.2. Exogenous spermine improved cardiac functions by lowering oxidative stress and apoptosis in T1D rats

To explore the effect of spermine on DCM, we administered spermine to the rats before and after STZ delivery, and then evaluated cardiac function at 12 weeks after STZ-injection. Supply of spermine significantly improved cardiac functions as measured by echocardiography in T1D rats (Fig. 1g). Spermine injection also attenuated the elevated level of GSP (Fig. 1k) and several serum cardiac markers in T1D rats, including CK-MB, cTnT, and LDH (Fig. 1h–j). In T1D rats, cardiomyocytes were disorderly arranged with dissolved nuclei, coagulative necrosis, and wavy myocardial fibers. Cardiomyocyte hypertrophy and nuclear malformation were also visible in the T1D group (Fig. 1l, H&E staining). Cardiac fibrosis and collagen deposition were notably increased in T1D rats, as detected by Masson's trichrome and Sirius Red staining (Fig. 1l and m). In contrast, the myocardium of spermine-injected T1D rats displayed minimal histological changes compared to control rats. We further examined the ultrastructure of cardiomyocytes by transmission electron microscopy (TEM). Rats receiving STZ injection developed dysplasia of sarcomere, rupture of myofilaments, disappearance of nuclei, and abnormal mitochondrial structure, all of which was minimally visible in spermine-injected T1D rats (Fig. 1l, TEM).

Myocardial injury is often associated with oxidative stress. In cardiac tissue homogenate from T1D rats, we detected a higher level of oxidative stress, indicated by decreased content of SOD2, lower activity of CAT, and increased content of lipid peroxidation product MDA. In contrast, these changes were markedly reversed by exogenous spermine in the myocardium (Fig. 1n–p). Nrf2 acts as a master regulator for oxidative stress [13]. We then detected that Nrf2 expression was decreased in myocardial tissues from T1D rats, which was significantly increased by spermine treatment (Supplementary Fig. 1a), suggesting that spermine may play an antioxidant role by activating Nrf2.

Furthermore, we observed increased cell apoptosis and ER stress in the hearts of T1D rats. Western blot data demonstrated that the protein expressions of apoptotic markers (cleaved caspases) and ER stress/unfolded protein response markers (Grp78 and Grp94) were significantly higher in T1D rats. Meanwhile, the expressions of the anti-apoptotic heat shock protein 70 (Hsp70) was decreased in T1D rat myocardium (Fig. 2a). Additional markers for stress-induced apoptosis, including MDM2, MDM4 and p53, were also upregulated in T1D rats (Fig. 2b and c). However, the expressions of these proteins or mRNAs in T1D rats received with spermine co-administration were similar to that of control level (Fig. 2c).

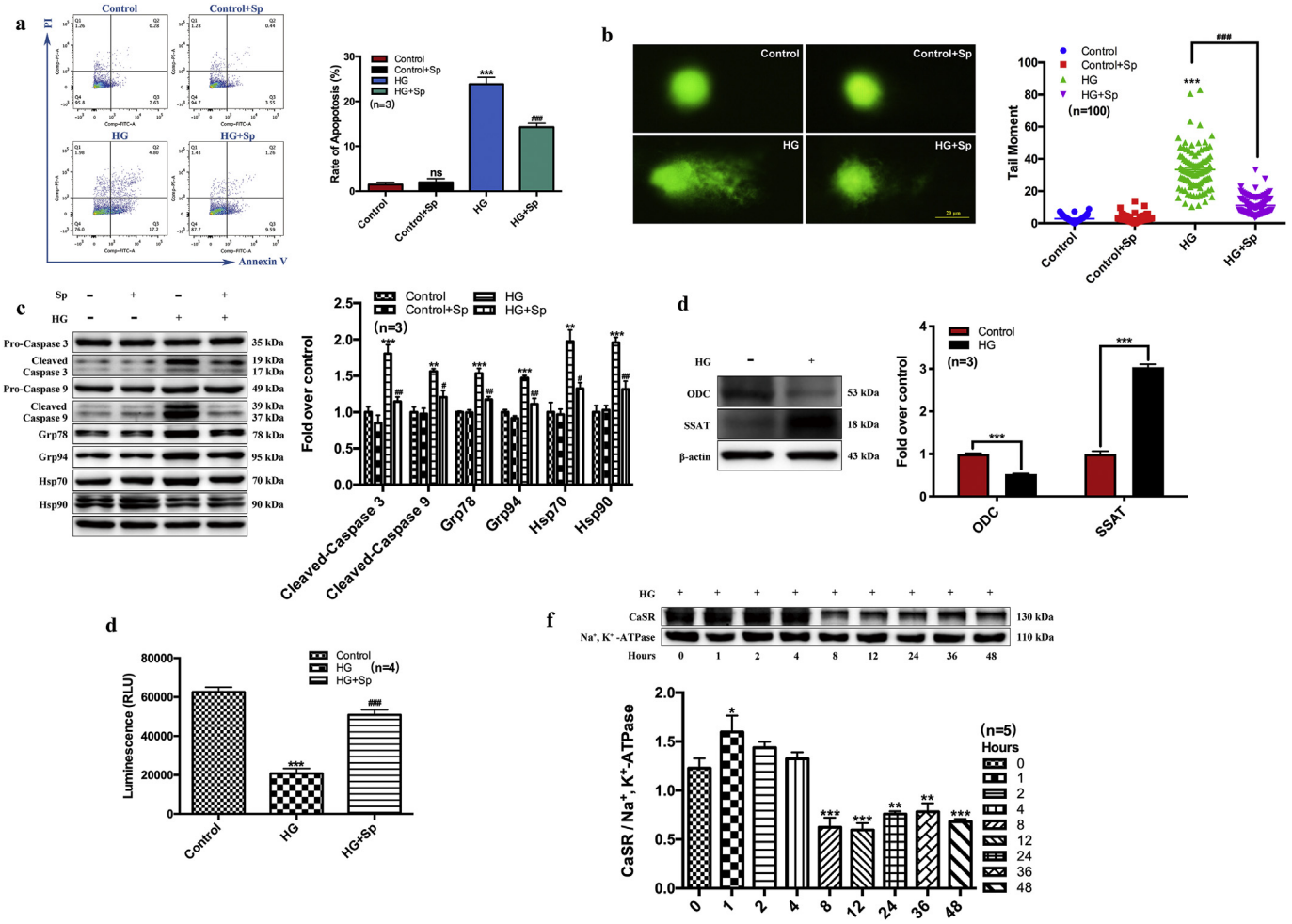

Fig. 3. HG induces cardiomyocyte apoptosis, decreases endogenous spermine content and expression of cytomembrane CaSR. We used 40 mmol/L HG to treat cardiomyocytes for 24 h *in vitro*. (a) Apoptosis rate was detected by flow cytometry, (b) DNA damage was detected by comet assay, (c) Quantification of apoptosis and ER stress related protein expression change, (d) Quantification of ODC and SSAT protein expression change, (e) Glucose uptake, and (f) CaSR expression changes were measured by western blot. Scale bar = 20 μm. *, P < 0.05 versus Control group; **, P < 0.01 versus Control group; ***, P < 0.001 versus Control group; #, P < 0.05 versus HG group; ##, P < 0.01 versus HG group; ###, P < 0.001 versus HG group.

3.3. Dysfunction of spermine metabolism-related enzymes and CaSR in the hearts from T1D rats

The level of intracellular spermine is under tight regulation by several proteins, including the synthetic enzyme ODC, SSAT and ODC antizyme (OAZ) [9]. In T1D rats, the cardiac expression of ODC was down-regulated but SSAT was up-regulated at both protein and mRNA levels (Fig. 2d and e). The expression of OAZ1 mRNA remained constant (Fig. 2e). Together, these results are indicative of a negative regulation of endogenous spermine content in T1D rat myocardium.

We have previously shown that HG-induced cardiomyocyte dysfunction *in vitro* was partially attributable to the down-regulation of myocardial CaSR expression and subsequent decrease in intracellular calcium concentration [6]. Likewise, in T1D rats, the mRNA expression and membrane content of myocardial CaSR was significantly reduced compared with control rats. The reduction was prevented by administration of exogenous spermine (Fig. 2f and g). Immunofluorescent staining located CaSR expression to the cell membrane of cardiomyocytes. The immunofluorescent signal of CaSR was significantly lower in T1D myocardium, while it was restored upon spermine pretreatment (Fig. 2h).

The correct folding and secretion of CaSR protein requires disulfide bond formation and stabilization by ER-resident oxidoreductases, mainly Ero1 and PDI [14]. In T1D rat cardiac tissue, the Ero1 and PDI mRNA was upregulated (Fig. 2g). Notably, Western blot showed that these upregulated enzymes skewed toward their reduced forms, which usually have impaired enzymatic activity in maintaining substrate disulfide bonds (Fig. 2f). Exogenous spermine prevented the upregulation of Ero1 and PDI mRNA, and restored the oxidized forms of both enzymes (Fig. 2g and f).

3.4. Exogenous spermine inhibited HG-induced apoptosis and ER stress in cultured neonatal rat cardiomyocytes

We next characterized the effect of exogenous spermine on myocardial injury *in vitro*. In primary cardiomyocytes isolated from neonatal rats, HG treatment markedly increased the apoptotic cell rate, as detected by flow cytometry analysis of apoptotic markers. Exogenous spermine had no effect on apoptosis at baseline, but significantly reversed HG-induced cardiomyocyte apoptosis (Fig. 3a). DNA double strand breakage is a hallmark of apoptosis. Using the Comet assay, we observed significantly prolonged comet tails in HG-treated cardiomyocyte nuclei. Co-treatment with exogenous spermine reduced the comet tail length close to control length (Fig. 3b). In HG-treated rat cardiomyocytes, we also observed shrinkage and vacuolization of mitochondria by TEM (Supplementary Fig. 2). However, the mitochondria in cells treated with exogenous spermine were morphologically indistinguishable from those in the control cells.

In view of the cardiac protein dysregulation in T1D rats, we examined the protein markers associated with apoptosis and ER stress in cultured neonatal rat cardiomyocytes by Western blot. In agreement with the *in vivo* data, exogenous spermine significantly attenuated HG-induced expressions of pro-apoptotic proteins and ER stress markers (Fig. 3c and Supplementary Fig. 3). We also determined the level of critical enzymes involved in spermine metabolism in neonatal rat cardiomyocytes. HG significantly reduced ODC expression but increased SSAT expression (Fig. 3d), an effect similar to that of T1D rats indicative of a negative balance of intracellular spermine. We then analyzed the cellular glycol-metabolism by a bioluminescent glucose uptake assay. The glucose uptake capacity was significantly impaired in HG-treated cardiomyocytes, but was restored by exogenous spermine treatment (Fig. 3e).

3.5. Exogenous spermine promoted CaSR synthesis and membrane localization by improving ER stress

We have previously shown that HG-induced down-regulation of myocardial CaSR contributed to cardiomyocyte dysfunction ex *vivo* [6]. Here, we further characterized cardiomyocyte membrane CaSR protein level *in vitro* at different time points following HG treatment. The cell membrane CaSR protein was increased at 1 h after HG treatment followed by a time-dependent decline to nearly half the baseline level at 8–12 h post-HG (Fig. 3f). In contrast, the decline of ODC protein expression was first detectable after 4–6 h HG treatment, whereas the increase of SSAT protein was first detectable after 12 h HG treatment (Supplementary Fig. 4). To explore the mechanisms underlying the change of cell membrane CaSR protein, we investigated the cardiac effect of exogenous spermine on CaSR expression, ER stress, and unfolded protein response (UPR), respectively. The signaling cascade of UPR pathway is dependent on 3 major transducers, including PERK, IRE1, and ATF6 [15]. We treated neonatal rat cardiomyocytes separately with UPR inhibitors specific to each transducer, and compared their effects on HG/spermine-regulated ER stress. GSK2606414 is a selective PERK inhibitor, STF-083010 is a specific IRE1 endonuclease inhibitor, and AEBSF HCl is a protease inhibitor targeting the transcription factor ATF6. Western blot showed the signaling proteins in all 3 major UPR pathways were markedly induced by HG treatment. Strikingly, exogenous spermine effectively suppressed UPR activation to levels comparable to specific UPR inhibitors (Fig. 4a–c). Besides with the specific inhibitors, we tested the effect of 4-phenylbutyric acid (4-PBA), a chemical chaperone that non-specifically eliminates UPR activity. Protein markers of ER stress, including Grp78, Grp94, and CHOP, were induced in HG-treated cardiomyocytes. However, exogenous spermine significantly suppressed these markers to a similar extent as 4-PBA (Fig. 4d). Taken together, these results strongly suggested that exogenous spermine inhibit HG-induced cardiac ER stress and UPR activation *in vitro*.

Notably, the suppression of UPR by exogenous spermine was associated with restored expression of CaSR protein on plasma membrane (Fig. 4d). Considering the possibility of ER stress impairing membrane protein synthesis and secretion, we examined the subcellular localization of CaSR in ER, cytoplasm and plasma membrane fractions by Western blot. We found that the expression of CaSR in HG-treated cardiomyocytes was significantly reduced in plasma membrane but increased in the cytoplasm (containing ER), consistent with a pattern of impaired ER-to-plasma-membrane transportation. Exogenous spermine restored the subcellular localization pattern of CaSR similar to control cells (Fig. 4e). These results suggest that exogenous spermine promotes CaSR synthesis and membrane localization by improving ER stress.

3.6. Exogenous spermine attenuated ROS generation by activating essential redox enzymes for CaSR synthesis

To better understand the protective mechanism of exogenous spermine, we measured ROS generation in neonatal rat cardiomyocytes by flow cytometry using DCFH-DA. HG treatment markedly increased intracellular ROS level. Exogenous spermine significantly lowered ROS generation in HG-treated cells. Treatment with NAC (an ROS scavenger) resulted in similar level of ROS reduction, further suggesting that exogenous spermine could prevent excessive ROS production by HG (Fig. 5a). It has been shown that Nrf2 inhibits the oxidative stress by activating SOD and CAT [16–18]. We next found that HG suppressed the protein expressions of both Nrf2 and SOD2, which were significantly upregulated by exogenous spermine (Supplemental Fig. 2b). siRNA-mediated knockdown of Nrf2 abolished the stimulatory role of spermine on the activities of SOD2 and CAT (Supplementary Figs. 1c–e). Consequently, the upregulation of protein markers of oxidative stress and DNA damage were uniformly attenuated by exogenous spermine similar to NAC treatment (Fig. 5b and c).

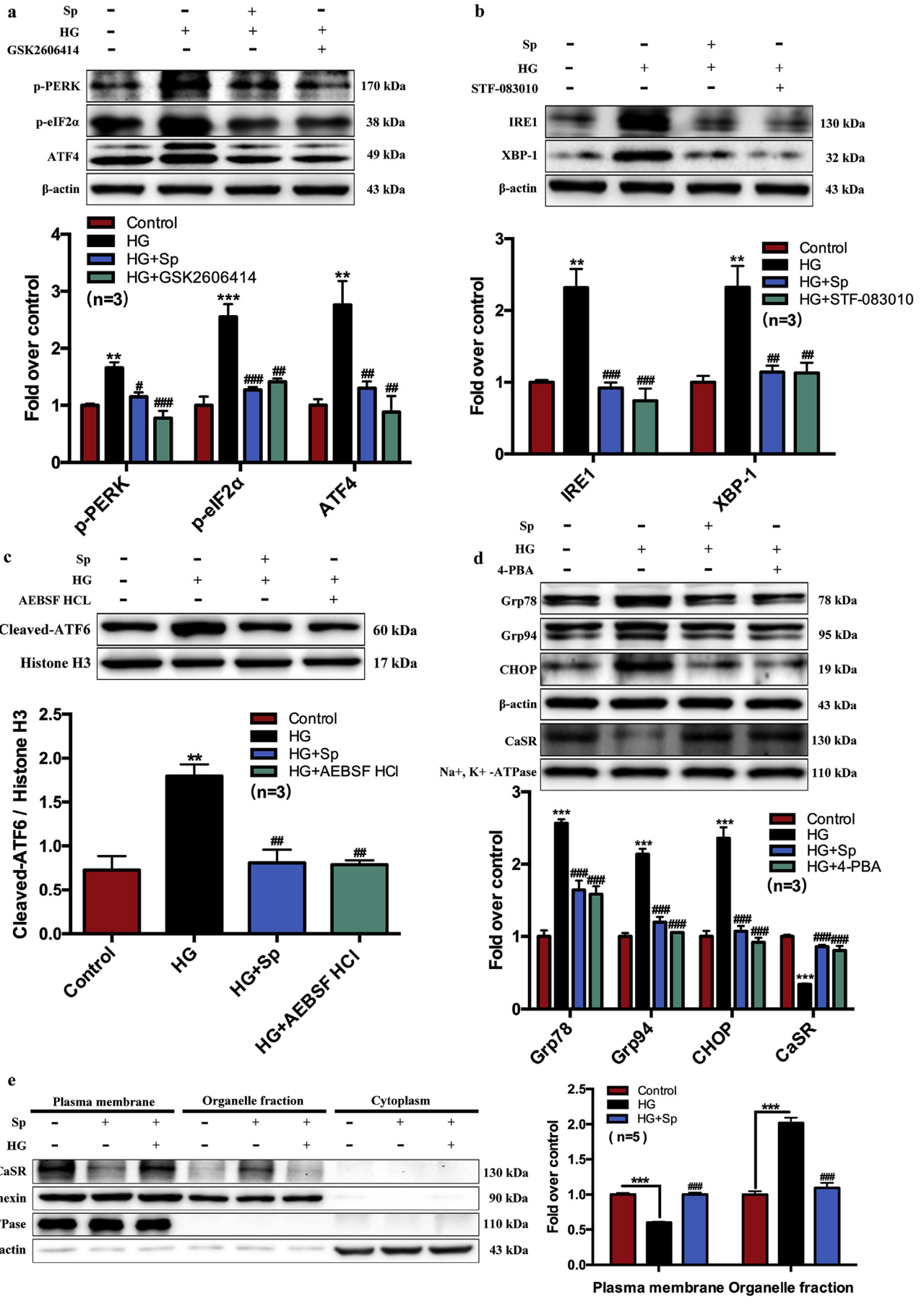

(caption on next page)

Fig. 4. Exogenous spermine up-regulates the expression of cytomembrane CaSR in cardiomyocytes by inhibiting ER stress. GSK2606414, STF-083010, AEBSF HCl, and 4-PBA were used to inhibit the ER stress. (a) The representative bands and quantification statistics of PERK signaling pathway, (b) The representative bands and quantification statistics of IRE1 signaling pathway, (c) The representative bands and quantification statistics of ATF6 signaling pathway, (d) The representative bands and quantification statistics of Grp78, Grp9, CHOP and cytomembrane CaSR protein expression, (e) The expression of CaSR in ER-cytoplasm-cytomembrane was detected by Western blot. **, P < 0.01 versus Control group; ***, P < 0.001 versus Control group; #, P < 0.05 versus HG group; ##, P < 0.01 versus HG group; ###, P < 0.001 versus HG group.

In agreement with the *in vivo* data, oxidative stress in HG-treated neonatal rat cardiomyocytes was associated with dysregulation of ER-resident oxidoreductases Ero1 and PDI, which were both polarized toward reduced forms (Fig. 5d). Plasma membrane CaSR expression was lower in HG-treated cells, presumably due to impaired Ero1 and PDI activity leading to less disulfide bond formation. Conversely, exogenous spermine, or direct scavenging of ROS by NAC, restored the oxidized forms of Ero1 and PDI, and increased cell membrane CaSR expression (Fig. 5d).

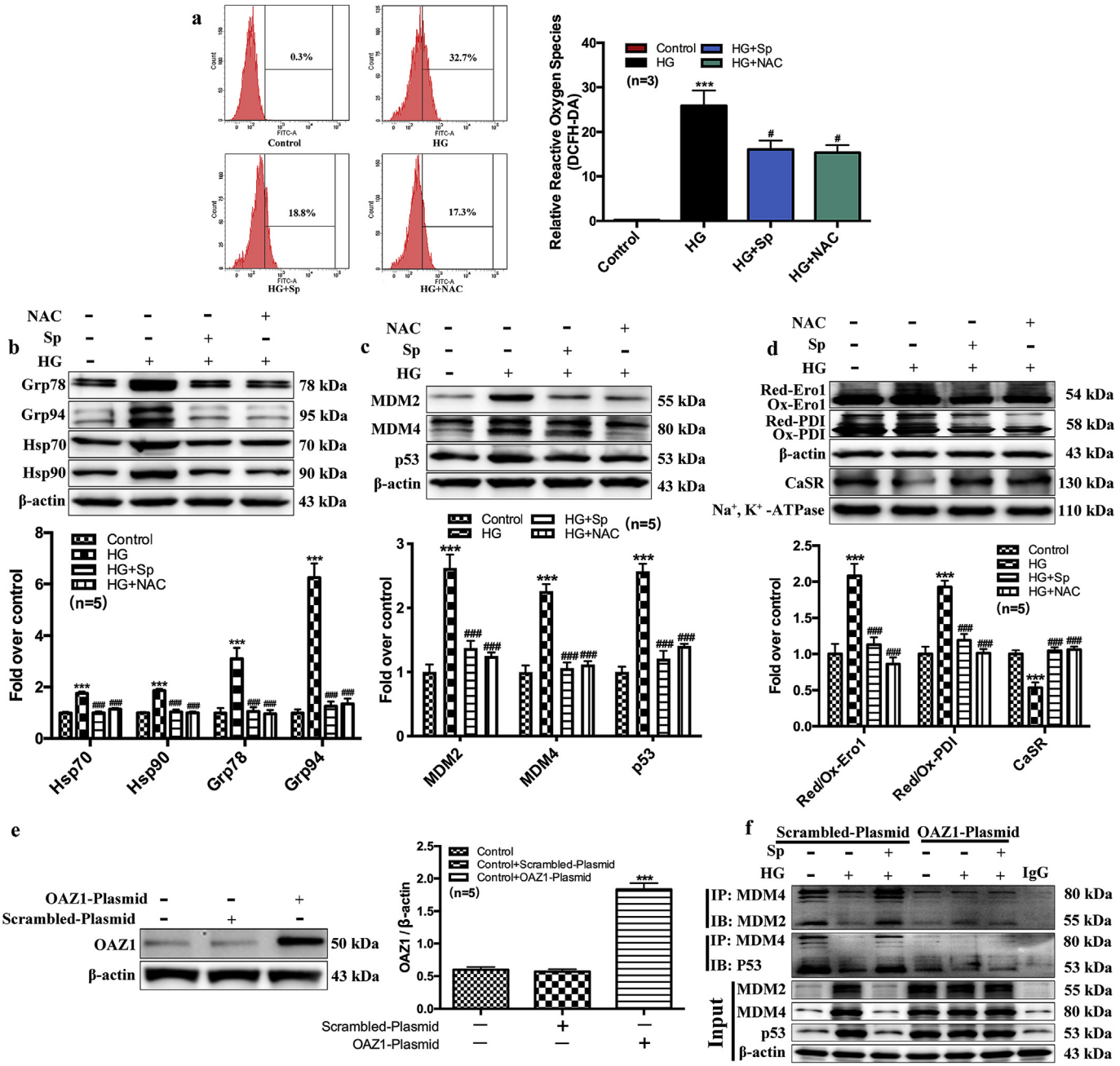

Fig. 5. Exogenous spermine protects cardiomyocytes by attenuating ROS level, stabilizing the redox state of cells, and up-regulating the expression of CaSR. By using NAC (ROS scavenger), we detected (a) The ROS level, (b) The expression of ER stress related proteins, (c) MDM2, MDM4 and p53 proteins and (d) CaSR synthesis related proteins. To further proved the effect of p53 on regulation of CaSR, OAZ1 overexpression was used. (e) Western blot was used to detect the overexpression efficiency of OAZ1, and (f) Immunoprecipitation was used to detect the formation of MDM4-MDM2 and MDM4-p53 complex. ***, P < 0.001 versus Control group; #, P < 0.05 versus HG group; ###, P < 0.001 versus HG group.

3.7. Exogenous spermine promoted plasma membrane CaSR expression by inhibiting the P53-MuRF1-PPAR α axis

We further explored additional mechanism that could potentially link to spermine-induced protection against HG-induced cardiac injury. OAZ1 is an enzyme that negatively regulates endogenous spermine level by binding to ODC for its degradation, as well as inhibiting exogenous polyamine uptake. We overexpressed OAZ1 enzyme in neonatal rat cardiomyocytes by delivering an OAZ1-plasmid (Fig. 5e). In control cardiomyocytes overexpressing scrambled plasmid, the protein interaction between MDM4 and MDM2, or MDM4 and p53 could be detected by immunoprecipitation, suggesting the possible inactivation of p53 by the MDM homologs. The protein complexes were decreased in HG-treated cells but restored by exogenous spermine treatment (Fig. 5f). In addition, exogenous spermine promoted the degradation of p53 (Fig. 5f). All these results are supportive of a protective role of p53 inactivation against HG-induced cardiac injury. In contrast, overexpression of OAZ1 led to diminished MDM4-MDM2 and MDM4-p53 complexes and minimal p53 degradation at all conditions (Fig. 5f). Meanwhile, plasma membrane CaSR expression was significantly decreased in OAZ1-overexpressing cardiomyocytes at baseline, and failed to increase after exposure to exogenous spermine (Fig. 6a). Together, these results suggested that the cardioprotective effect of exogenous spermine and membrane CaSR expression were both dependent upon p53 inactivation, and that enzymatic inactivation of endogenous spermine synthesis could diminish such cardioprotective effects.

MuRF1 is an effector ubiquitin ligase targeting myofibrils for degradation [19,20]. We knocked-down the endogenous MuRF1 in cardiomyocytes by using siRNA or over-expressed MuRF1 by an exogenous MuRF1-plasmid (Fig. 6b–g). In cells receiving non-targeting vectors, MuRF1 was marked upregulated by HG and reduced by exogenous spermine treatment. The expression of MuRF1 was conversely correlated with the expression of PPARα and CaSR, consistent with its known effector role leading to protein degradation and myocardial atrophy (Fig. 6c–g). Silencing of MuRF1 prevented HG-induced degradation of PPARα and CaSR (Fig. 6c and d), whereas overexpression of MuRF1 accelerated CaSR degradation at all condition, even in the absence of HG treatment (Fig. 6f and g).

Surprisingly, MuRF1-induced CaSR degradation can be counteracted by exogenous PPARα protein (Fig. 6f and g). Therefore, we focused on the role of PPARα in HG-induced cardiac injury by silencing or overexpressing PPARα (Fig. 7). In contrast to prior *in vivo* (Fig. 2f and g) and *in vitro* data (Fig. 5d), silencing endogenous PPARα abolished the capacity of exogenous spermine to maintain oxidized forms of Ero1 and PDI followed by stable expression of membrane CaSR (Fig. 7a–c). In contrast, overexpression of PPARα decreased HG-induced cardiomyocyte ROS production, comparable to exogenous spermine treatment (Fig. 7d). Overexpression of PPARα also upregulated membrane expression of CaSR in response to exogenous spermine treatment (Fig. 7e).

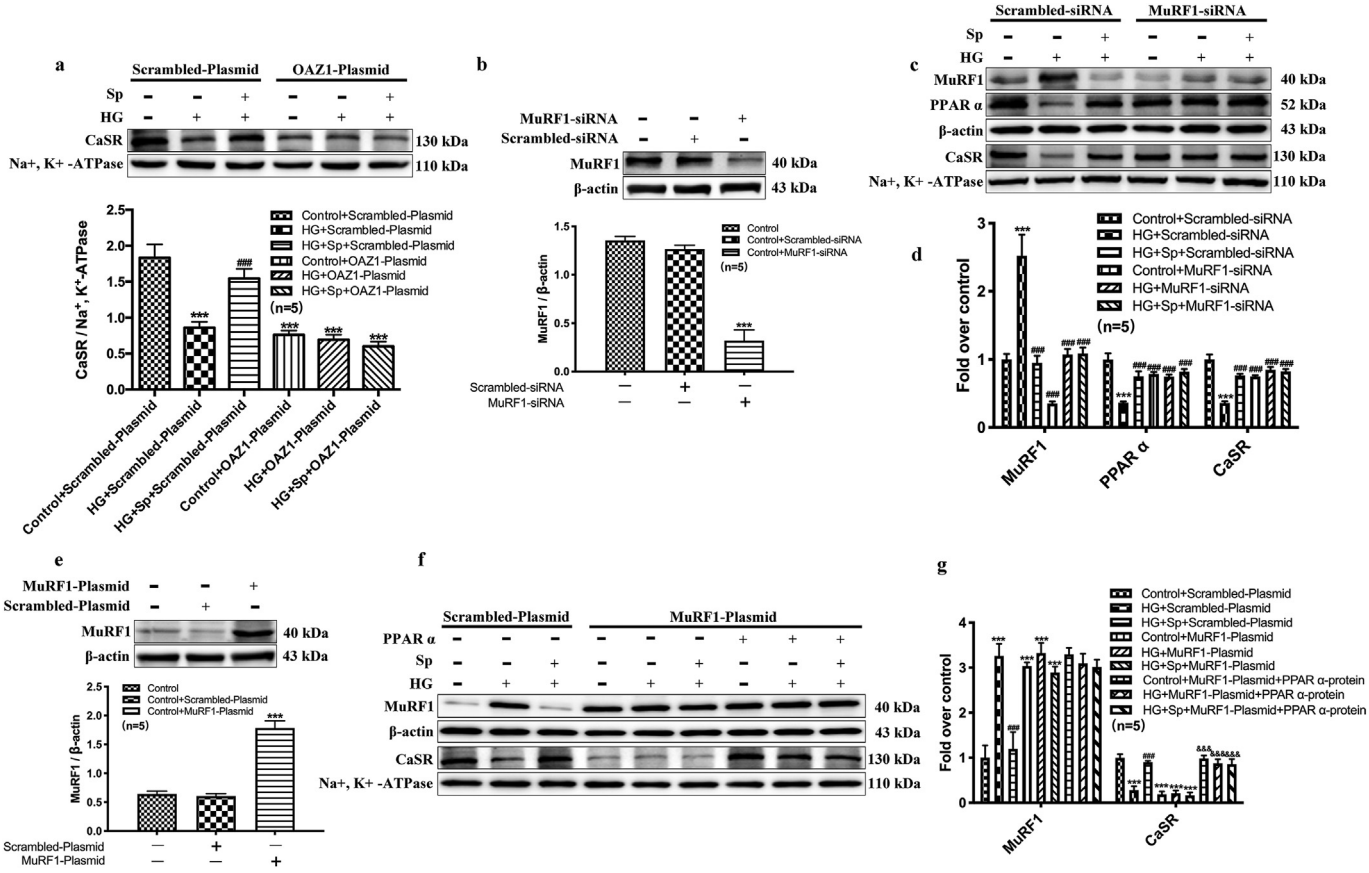

Fig. 6. p53 inhibits PPARα expression by activating MuRF1, which can affect the process of CaSR synthesis. (a) The effect of OAZ1 overexpression on the cytomembrane CaSR expression. MuRF1-siRNA was used to transfect cardiomyocytes to verify its involvement in regulating cytomembrane CaSR synthesis, and (b) Western blot was used to detect the transfect efficiency of MuRF1-siRNA, the representative band and quantification of MuRF1 expression was shown, (c) The representative bands of MuRF1, PPARα and CaSR expression change, (d) Quantification of MuRF1, PPAR α and CaSR expression statistics. (e) Western blot was used to detect the overexpression efficiency of MuRF1, the representative band and quantification of MuRF1 expression was shown, (f) The representative bands of MuRF1 and CaSR expression change, and (g) Quantification of MuRF1 and CaSR expression statistics. ***, P < 0.001 versus Control group or Control + Scrambled-siRNA group or Control + Scrambled-Plasmid group; ###, P < 0.001 versus HG + Scrambled-siRNA group or HG + Scrambled-Plasmid group; &&&, P < 0.001 versus HG + MuRF1-Plasmid group.

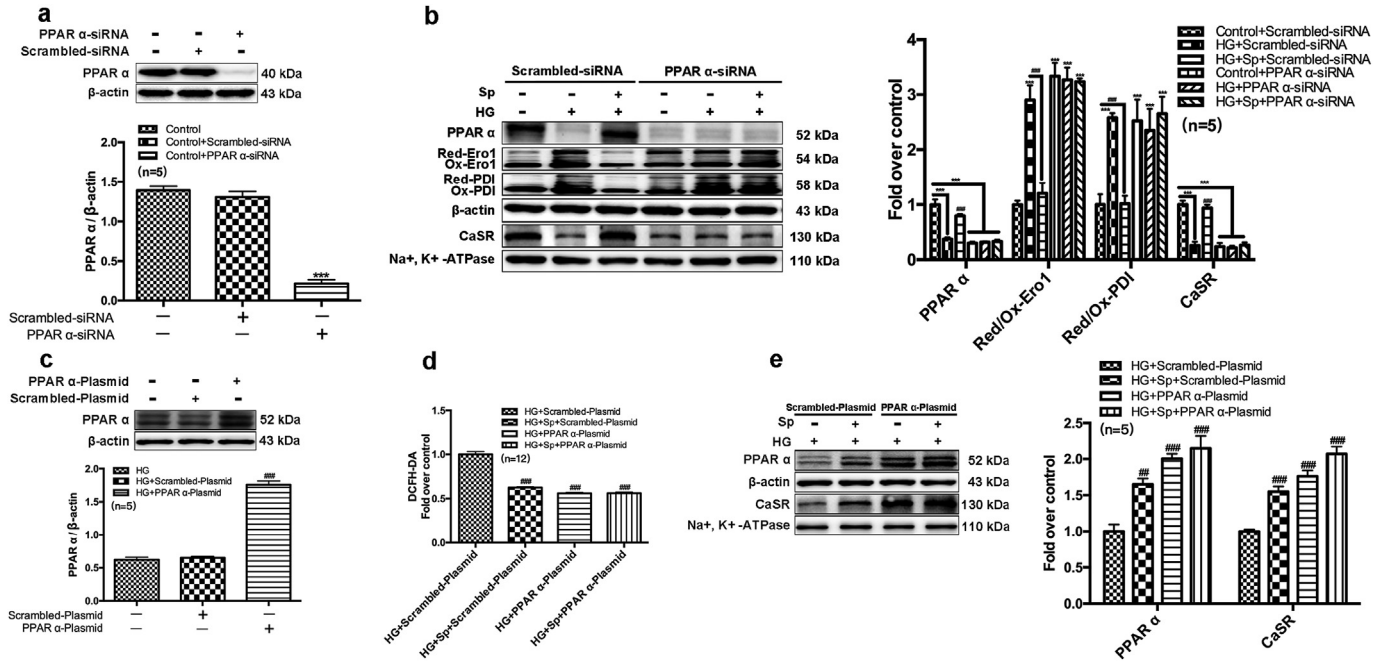

Fig. 7. PPARα participates in the synthesis of CaSR by inhibiting ROS. (a) Western blot was used to detect the transfect efficiency of PPAR α-siRNA, the representative band and quantification of PPAR α protein expression was shown, (b) The representative band and quantification of PPARα, Ero1, PDI and CaSR protein expression change were shown, (c) Western blot analysis of the PPARα overexpression efficiency, the representative band and quantification of PPARα protein expression was shown, (d) Quantification of intracellular ROS level statistics, (e) The representative bands of PPARα and CaSR protein expression change and quantification of PPARα and CaSR protein expression statistics. ***, P < 0.001 versus Control group or Control + Scrambled-siRNA group; ##, P < 0.01 versus HG + Scrambled-Plasmid group; ###, P < 0.001 versus HG group or HG + Scrambled-siRNA group or HG + Scrambled-Plasmid group.

4. Discussion

The major finding of this study is that exogenous spermine protects against DCM *in vivo* and *in vitro*, partially by suppressing ROS- and p53-mediated downregulation of CaSR in cardiomyocytes. Exogenous spermine attenuated cardiac dysfunction in T1D rats, alleviated HG-induced ROS level and ER stress, and inhibited several downstream effector pathways causing DCM, including dysregulation of calcium

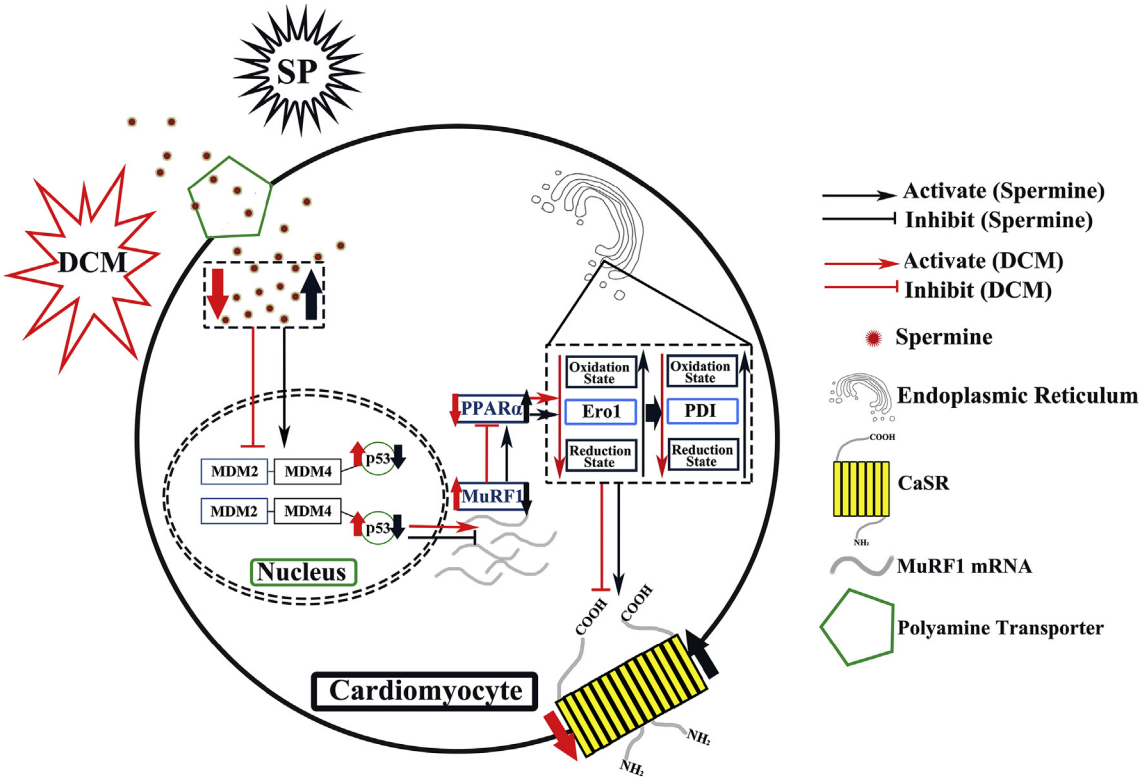

Fig. 8. A proposed theoretical model of spermine regulation of cytomembrane CaSR synthesis.

homeostasis secondary to CaSR reduction, activation of MuRF1, and inhibition of PPARα (Fig. 8).

DCM is a common and severe complication of T1D with an increased incidence rate globally [1,21]. Cardiac dysfunction caused by DCM manifests early in T1D, contributing to the early morbidity and high mortality of T1D patients [22,23]. There is no cure for DCM at present and clinical trials for DCM therapy have largely been unsatisfactory [24-26]. Therefore, finding novel therapeutic strategies for DCM remains an urgent public health need. By using a chemically induced-T1D model, we confirmed that STZ damaged cardiac dysfunctions and lead to hyperglycemia, hyperlipidemia, hypoinsulinemia, and decreased body weight in rats. We previously have shown that metabolic imbalance of polyamine is related to a variety of disorders including diabetes, neurodegenerative changes, and myocardial ischemia reperfusion injury [27–29]. Spermine is an important polyamine involved in cellular metabolism found in all mammalian cells, however the roles of spermine in DCM is not clear. The present data showed the critical roles of spermine in protecting DCM [30]. First, spermine plays an essential role in regulating myocardial functions by maintaining the expression of membrane CaSR. Other studies also reported that exogenous spermine could be a non-specific agonist of CaSR [6]. Our data further showed that loss of membrane CaSR in DCM was associated with decreased expression of spermine synthetic enzyme ODC and increased expression of catabolic enzyme SSAT. Importantly, we revealed that the decreased membrane CaSR was secondary to endogenous spermine deficiency, as evidenced by the occurrence of ODC decrease at 4–6 h followed by membrane CaSR decrease at 8 h. SSAT began to increase at 12 h, which would further facilitate the degradation of spermine. These results indicate that spermine may function not only as a direct CaSR agonist, but also as a regulator of CaSR synthesis and degradation. In addition, cardiac PPARα was found to mediate spermine-dependent membrane CaSR expression, indicating a key connection between metabolic change and calcium homeostasis via spermine in regulating cardiac functions.

Spermine is known as a ROS scavenger and is capable of protecting DNA from free radical attack [31]. ROS is closely related to ER stress and mitochondrial damage. Exogenous spermine has been shown to inhibit ER stress-induced apoptosis of primary neonatal rat cardiomyocytes via reducing the production of ROS and inhibiting the activation of PERK-eIF2α and p38-JNK pathway [27,28]. Spermine also reduced the permeability of mitochondria, inhibited the leakage of mitochondrial glutathione, and prevented mitochondrial swelling [6,32–34]. In addition to its direct antioxidant actions, spermine was also able to stimulate Nrf2, a master transcription factor in regulating the expression of antioxidant genes, including SODs and CAT [35–37]. Consistent with these discoveries, our results strongly support that the anti-oxidant activity of spermine is essential to its cardioprotective effect [27,28,38,39]. First, the improvement of cardiac functions in T1D rats by exogenous spermine was associated with lower cardiac oxidative stress. Second, the cardioprotective effect of exogenous spermine can be fully replicated by ROS scavenger in cardiomyocytes. In other words, exogenous spermine can inhibit the accumulation of ROS *in vitro* and *in vivo* by acting as a ROS scavenger (directly) and activating Nrf2 (indirectly). Third, spermine restored the oxidatized forms of 2 ER oxidoreductases (Ero1 and PDI), which are critical for proper folding and secretion of CaSR.

Our results highlighted several critical downstream effector pathways of DCM and HG-induced cardiomyocyte injury, which are effectively targeted by exogenous spermine. First, ER stress and subsequent UPR appear to be central for the development of DCM *in vivo* and HG-induced myocardial dysfunction *in vitro*. ER stress and UPR can be induced by excessive ROS [40], which was evident in DCM and HG-treated cells. Grp78 and Grp94 are important molecular chaperones in ER and act as core regulators of UPR [41]. HG treatment markedly upregulated the expressions of Grp78 and Grp94 indicative of enhanced UPR, which in turn led to abnormal protein synthesis and apoptosis. Conversely, cardiomyocytes treated with UPR inhibitors (GSK2606414, STF-083010, AEBSF HCL and 4-PBA) could essentially recapitulate the protective effect of exogenous spermine, demonstrating the importance of UPR in DCM and the cardioprotection by spermine. Second, p53 activation is clearly implicated in HG-induced myocardial dysfunction. p53 is a core member of cellular DNA damage responses, which is evident in the HG group shown by the neutral comet assays [42]. Under physiological conditions, MDM2 and MDM4 induced ubiquitination of p53 and thereby inhibit p53 [43]. Our results showed that MDM2 and MDM4 levels were elevated in heart of T1D rats and HG-treated cardiomyocytes, a likely feedback response to elevated p53 following DNA damage [44]. Despite the increased protein expression, MDM4-p53 interaction was diminished in response to HG, potentially accounting for activation of p53 and apoptosis. Of note, p53 serves as a “hub” that connects a wide range of important effectors. For instance, DNA damage caused by HG can lead to increased p53, which promotes a significant shift of Ero1 and PDI towards their reduced state. p53 also binds to the promoter of the gene encoding MuRF1 and promotes its transcription [19]. Third, our data revealed a novel role of MuRF1 in DCM that has never been reported. MuRF1 has been previously implicated in cardiac remodeling following myocardial infarction and ischemia reperfusion injury [45,46]. The present results showed that myocardial MuRF1 was up-regulated in response to HG incubation. Silencing of MuRF1 up-regulated PPARα and CaSR, whereas overexpression of MuRF1 aggravated HG-induced injury and abolished the protective effect of exogenous spermine. These data suggest that MuRF1 could therefore serve as a novel indicator for myocardial injury or response to therapy.

In conclusion, the present data demonstrated that the accumulation of ROS and Ero1/PDI redox state unbalance caused by the decreased spermine would lead to abnormal synthesis of membrane CaSR in DCM. Supplement of spermine can inhibit the cell damage caused by higher ROS production and ER stress under DCM conditions. Application of exogenous spermine may represent a novel therapeutic strategy in managing DCM in T1D.

Declaration of competing interest

The author(s) declared no potential conflicts of interest with respect to the research, authorship, and/or publication of this article.

Acknowledgments

Hereby, we are very grateful to all colleagues in the Department of Pathophysiology, College of Basic Medicine, Harbin Medical University for their selfless help during the period of our study. YHW and CW designed the research and drafted the manuscript; YHW, JTC, SWL, XYZ, ZMG and NYS completed the experiment and data analysis; JH and XTS fed the animals and prepared diabetes model; HZL, YJZ, GDY, and CQX revised the paper and gave some suggestions. All authors reviewed the results and approved the final version of the manuscript.

Appendix A. Supplementary data

Supplementary data to this article can be found online at https://doi.org/10.1016/j.redox.2020.101514.

Funding

This research is supported by the National Natural Science Foundation of China (No. 81800260) and Heilongjiang Postdoctoral Fund (No. LBH-Z17103).

References

[1] E.A. Gale, Type 1 diabetes in the young: the harvest of sorrow goes on, Diabetologia 48 (8) (2005) 1435–1438.

[2] M. Battaglia, M.S. Anderson, J.H. Buckner, S.M. Geyer, P.A. Gottlieb, T.W.H. Kay, A. Lernmark, S. Muller, A. Pugliese, B.O. Roep, C.J. Greenbaum, M. Peakman, Understanding and preventing type 1 diabetes through the unique working model of TrialNet, Diabetologia 60 (11) (2017) 2139–2147.

[3] S. Rubler, J. Dlugash, Y.Z. Yuceoglu, T. Kumral, A.W. Branwood, A. Grishman, New type of cardiomyopathy associated with diabetic glomerulosclerosis, Am. J. Cardiol. 30 (6) (1972) 595–602.

[4] B.R. Goyal, A.A. Mehta, Diabetic cardiomyopathy: pathophysiological mechanisms and cardiac dysfuntion, Hum. Exp. Toxicol. 32 (6) (2013) 571–590.

[5] D.C. Raev, Which left ventricular function is impaired earlier in the evolution of diabetic cardiomyopathy? An echocardiographic study of young type I diabetic patients, Diabetes Care 17 (7) (1994) 633–639.

[6] Y. Wang, P. Gao, C. Wei, H. Li, L. Zhang, Y. Zhao, B. Wu, Y. Tian, W. Zhang, L. Wu, R. Wang, C. Xu, Calcium sensing receptor protects high glucose-induced energy metabolism disorder via blocking gp78-ubiquitin proteasome pathway, Cell Death Dis. 8 (5) (2017) e2799.

[7] S.Z. Bai, J. Sun, H. Wu, N. Zhang, H.X. Li, G.W. Li, H.Z. Li, W. He, W.H. Zhang, Y.J. Zhao, L.N. Wang, Y. Tian, B.F. Yang, G.D. Yang, L.Y. Wu, R. Wang, C.Q. Xu, Decrease in calcium-sensing receptor in the progress of diabetic cardiomyopathy, Diabetes Res. Clin. Pract. 95 (3) (2012) 378–385.

[8] W.H. Zhang, S.B. Fu, F.H. Lu, B. Wu, D.M. Gong, Z.W. Pan, Y.J. Lv, Y.J. Zhao, Q.F. Li, R. Wang, B.F. Yang, C.Q. Xu, Involvement of calcium-sensing receptor in ischemia/reperfusion-induced apoptosis in rat cardiomyocytes, Biochem. Biophys. Res. Commun. 347 (4) (2006) 872–881.

[9] A.E. Pegg, Mammalian polyamine metabolism and function, IUBMB Life 61 (9) (2009) 880–894.

[10] R.M. Adibhatla, J.F. Hatcher, K. Sailor, R.J. Dempsey, Polyamines and central nervous system injury: spermine and spermidine decrease following transient focal cerebral ischemia in spontaneously hypertensive rats, Brain Res. 938 (1–2) (2002) 81–86.

[11] J. Wu, Z. Tian, Y. Sun, C. Lu, N. Liu, Z. Gao, L. Zhang, S. Dong, F. Yang, X. Zhong, C. Xu, F. Lu, W. Zhang, Exogenous H_2S facilitating ubiquitin aggregates clearance via autophagy attenuates type 2 diabetes-induced cardiomyopathy, Cell Death Dis. 8 (8) (2017) e2992.

[12] E. Patterson, T.M. Marques, O. O'Sullivan, P. Fitzgerald, G.F. Fitzgerald, P.D. Cotter, T.G. Dinan, J.F. Cryan, C. Stanton, R.P. Ross, Streptozotocin-induced type-1-diabetes disease onset in Sprague-Dawley rats is associated with an altered intestinal microbiota composition and decreased diversity, Microbiology 161 (Pt 1) (2015) 182–193.

[13] Y. Tong, S. Liu, R. Gong, L. Zhong, X. Duan, Y. Zhu, Ethyl vanillin protects against kidney injury in diabetic nephropathy by inhibiting oxidative stress and apoptosis, Oxid Med Cell Longev 2019 (2019) 2129350.

[14] M.G. Pollard, K.J. Travers, J.S. Weissman, Ero1p: a novel and ubiquitous protein with an essential role in oxidative protein folding in the endoplasmic reticulum, Mol. Cell. 1 (2) (1998) 171–182.

[15] D.T. Rutkowski, R.J. Kaufman, A trip to the ER: coping with stress, Trends Cell Biol. 14 (1) (2004) 20–28.

[16] A. Shi, H. Shi, Y. Wang, X. Liu, Y. Cheng, H. Li, H. Zhao, S. Wang, L. Dong, Activation of Nrf2 pathway and inhibition of NLRP3 inflammasome activation contribute to the protective effect of chlorogenic acid on acute liver injury, Int. Immunopharm. 54 (2018) 125–130.

[17] G. Yang, K. Zhao, Y. Ju, S. Mani, Q. Cao, S. Puukila, N. Khaper, L. Wu, R. Wang, Hydrogen sulfide protects against cellular senescence via S-sulfhydration of Keap1 and activation of Nrf2, Antioxidants Redox Signal. 18 (15) (2013) 1906–1919.

[18] K. Yamada, K. Asai, F. Nagayasu, K. Sato, N. Ijiri, N. Yoshii, Y. Imahashi, T. Watanabe, Y. Tochino, H. Kanazawa, K. Hirata, Impaired nuclear factor erythroid 2-related factor 2 expression increases apoptosis of airway epithelial cells in patients with chronic obstructive pulmonary disease due to cigarette smoking, BMC Pulm. Med. 16 (2016) 27.

[19] Y. von Grabowiecki, P. Abreu, O. Blanchard, L. Palamiuc, S. Benosman, S. Meriaux, V. Devignot, I. Gross, G. Mellitzer, J.L. Gonzalez de Aguilar, C. Gaiddon, Transcriptional activator TAp63 is upregulated in muscular atrophy during ALS and induces the pro-atrophic ubiquitin ligase Trim63, Elife 5 (2016).

[20] O. Rom, A.Z. Reznick, The role of E3 ubiquitin-ligases MuRF-1 and MAFbx in loss of skeletal muscle mass, Free Radic. Biol. Med. 98 (2016) 218–230.

[21] Guidelines on Second-And Third-Line Medicines and Type of Insulin for the Control of Blood Glucose Levels in Non-pregnant Adults with Diabetes Mellitus, 2018 Geneva.

[22] K.J. Nadeau, J.G. Regensteiner, T.A. Bauer, M.S. Brown, J.L. Dorosz, A. Hull, P. Zeitler, B. Draznin, J.E. Reusch, Insulin resistance in adolescents with type 1 diabetes and its relationship to cardiovascular function, J. Clin. Endocrinol. Metab. 95 (2) (2010) 513–521.

[23] P. Bjornstad, U. Truong, L. Pyle, J.L. Dorosz, M. Cree-Green, A. Baumgartner, G. Coe, J.G. Regensteiner, J.E. Reusch, K.J. Nadeau, Youth with type 1 diabetes have worse strain and less pronounced sex differences in early echocardiographic markers of diabetic cardiomyopathy compared to their normoglycemic peers: a RESistance to InSulin in Type 1 ANd Type 2 diabetes (RESISTANT) Study, J. Diabet. Complicat. 30 (6) (2016) 1103–1110.

[24] N. Dickert, J. Sugarman, Ethical goals of community consultation in research, Am. J. Publ. Health 95 (7) (2005) 1123–1127.

[25] P. Bjornstad, M. Schafer, U. Truong, M. Cree-Green, L. Pyle, A. Baumgartner, Y. Garcia Reyes, A. Maniatis, S. Nayak, R.P. Wadwa, L.P. Browne, J.E.B. Reusch, K.J. Nadeau, Metformin improves insulin sensitivity and vascular health in youth with type 1 diabetes mellitus, Circulation 138 (25) (2018) 2895–2907.

[26] B. Parim, V.V. Sathibabu Uddandrao, G. Saravanan, Diabetic cardiomyopathy: molecular mechanisms, detrimental effects of conventional treatment, and beneficial effects of natural therapy, Heart Fail. Rev. 24 (2) (2019) 279–299.

[27] Y. He, J. Yang, H. Li, H. Shao, C. Wei, Y. Wang, M. Li, C. Xu, Exogenous spermine ameliorates high glucose-induced cardiomyocytic apoptosis via decreasing reactive oxygen species accumulation through inhibiting p38/JNK and JAK2 pathways, Int. J. Clin. Exp. Pathol. 8 (12) (2015) 15537–15549.

[28] C. Wei, Y. Wang, M. Li, H. Li, X. Lu, H. Shao, C. Xu, Spermine inhibits endoplasmic reticulum stress-induced apoptosis: a new strategy to prevent cardiomyocyte apoptosis, Cell. Physiol. Biochem. 38 (2) (2016) 531–544.

[29] T. Murray-Stewart, M. Dunworth, J.R. Foley, C.E. Schwartz, R.A. Casero Jr., Polyamine homeostasis in snyder-robinson syndrome, Med Sci (Basel) 6 (4) (2018).

[30] C.A. Guo, S. Guo, Insulin receptor substrate signaling controls cardiac energy metabolism and heart failure, J. Endocrinol. 233 (3) (2017) R131–R143.

[31] H.C. Ha, N.S. Sirisoma, P. Kuppusamy, J.L. Zweier, P.M. Woster, R.A. Casero Jr., The natural polyamine spermine functions directly as a free radical scavenger, Proc. Natl. Acad. Sci. U. S. A. 95 (19) (1998) 11140–11145.

[32] M.P. Rigobello, A. Toninello, D. Siliprandi, A. Bindoli, Effect of spermine on mitochondrial glutathione release, Biochem. Biophys. Res. Commun. 194 (3) (1993) 1276–1281.

[33] L. Xue, X. Liu, Q. Wang, C.Q. Liu, Y. Chen, W. Jia, R. Hsie, Y. Chen, F. Luh, S. Zheng, Y. Yen, Ribonucleotide reductase subunit M2B deficiency leads to mitochondrial permeability transition pore opening and is associated with aggressive clinicopathologic manifestations of breast cancer, Am J Transl Res 10 (11) (2018) 3635–3649.

[34] I.G. Sava, V. Battaglia, C.A. Rossi, M. Salvi, A. Toninello, Free radical scavenging action of the natural polyamine spermine in rat liver mitochondria, Free Radic. Biol. Med. 41 (8) (2006) 1272–1281.

[35] W. Cao, X. Xu, G. Jia, H. Zhao, X. Chen, C. Wu, J. Tang, J. Wang, J. Cai, G. Liu, Roles of spermine in modulating the antioxidant status and Nrf2 signalling molecules expression in the thymus and spleen of suckling piglets-new insight, J. Anim. Physiol. Anim. Nutr. 102 (1) (2018) e183–e192.

[36] C. Zhu, Y. Zhao, X. Wu, C. Qiang, J. Liu, J. Shi, J. Gou, D. Pei, A. Li, The therapeutic role of baicalein in combating experimental periodontitis with diabetes via Nrf2 antioxidant signaling pathway, J. Periodontal. Res. (2019), https://doi.org/10.1111/jre.12722.

[37] B. D'Autreaux, M.B. Toledano, ROS as signalling molecules: mechanisms that generate specificity in ROS homeostasis, Nat. Rev. Mol. Cell Biol. 8 (10) (2007) 813–824.

[38] C. Wei, H. Li, Y. Wang, X. Peng, H. Shao, H. Li, S. Bai, C. Xu, Exogenous spermine inhibits hypoxia/ischemia-induced myocardial apoptosis via regulation of mitochondrial permeability transition pore and associated pathways, Exp. Biol. Med. 241 (14) (2016) 1505–1515.

[39] C. Wei, H.Z. Li, Y.H. Wang, X. Peng, H.J. Shao, H.X. Li, S.Z. Bai, X.X. Lu, L.Y. Wu, R. Wang, C.Q. Xu, Exogenous spermine inhibits the proliferation of human pulmonary artery smooth muscle cells caused by chemically-induced hypoxia via the suppression of the ERK1/2- and PI3K/AKT-associated pathways, Int. J. Mol. Med. 37 (1) (2016) 39–46.

[40] A.H. Amin, M.A. El-Missiry, A.I. Othman, Melatonin ameliorates metabolic risk factors, modulates apoptotic proteins, and protects the rat heart against diabetes-induced apoptosis, Eur. J. Pharmacol. 747 (2015) 166–173.

[41] G. Zhu, A.S. Lee, Role of the unfolded protein response, GRP78 and GRP94 in organ homeostasis, J. Cell. Physiol. 230 (7) (2015) 1413–1420.

[42] D. Speidel, The role of DNA damage responses in p53 biology, Arch. Toxicol. 89 (4) (2015) 501–517.

[43] M. Yokoyama, I. Shimizu, A. Nagasawa, Y. Yoshida, G. Katsuumi, T. Wakasugi, Y. Hayashi, R. Ikegami, M. Suda, Y. Ota, S. Okada, M. Fruttiger, Y. Kobayashi, M. Tsuchida, Y. Kubota, T. Minamino, p53 plays a crucial role in endothelial dysfunction associated with hyperglycemia and ischemia, J. Mol. Cell. Cardiol. 129 (2019) 105–117.

[44] X. Li, K.K. Cheng, Z. Liu, J.K. Yang, B. Wang, X. Jiang, Y. Zhou, P. Hallenborg, R.L. Hoo, K.S. Lam, Y. Ikeda, X. Gao, A. Xu, The MDM2-p53-pyruvate carboxylase signalling axis couples mitochondrial metabolism to glucose-stimulated insulin secretion in pancreatic beta-cells, Nat. Commun. 7 (2016) 11740.

[45] E. Castillero, H. Akashi, C. Wang, M. Najjar, R. Ji, P.J. Kennel, H.L. Sweeney, P.C. Schulze, I. George, Cardiac myostatin upregulation occurs immediately after myocardial ischemia and is involved in skeletal muscle activation of atrophy, Biochem. Biophys. Res. Commun. 457 (1) (2015) 106–111.

[46] V.M. Conraads, C.J. Vrints, I.E. Rodrigus, V.Y. Hoymans, E.M. Van Craenenbroeck, J. Bosmans, M.J. Claeys, P. Van Herck, A. Linke, G. Schuler, V. Adams, Depressed expression of MuRF1 and MAFbx in areas remote of recent myocardial infarction: a mechanism contributing to myocardial remodeling? Basic Res. Cardiol. 105 (2) (2010) 219–226.